







RESEARCH ARTICLE

Brain network dynamics in people with visual snow syndrome

Myrte Strik¹  | Meaghan Clough² | Emma J. Solly²  | Rebecca Glarin¹  |
Owen B. White²  | Scott C. Kolbe²  | Joanne Fielding² 

¹Melbourne Brain Centre Imaging Unit, Department of Radiology, Melbourne Medical School, University of Melbourne, Melbourne, Victoria, Australia

²Department of Neuroscience, Central Clinical School, Monash University, Melbourne, Victoria, Australia

Correspondence

Myrte Strik, Melbourne Brain Centre Imaging Unit, Department of Radiology, Melbourne Medical School, The University of Melbourne, Level 1, Kenneth Myer Building, 30 Royal Parade, Parkville, VIC 3010 Australia.
Email: mstrik@unimelb.edu.au

Funding information

Visual Snow Initiative; Siemens Healthineers; University of Melbourne; MASSIVE HPC facility

Abstract

Visual snow syndrome (VSS) is a neurological disorder characterized by a range of continuous visual disturbances. Little is known about the functional pathological mechanisms underlying VSS and their effect on brain network topology, studied using high-resolution resting-state (RS) 7 T MRI. Forty VSS patients and 60 healthy controls underwent RS MRI. Functional connectivity matrices were calculated, and global efficiency (network integration), modularity (network segregation), local efficiency (LE, connectedness neighbors) and eigenvector centrality (significance node in network) were derived using a dynamic approach (temporal fluctuations during acquisition). Network measures were compared between groups, with regions of significant difference correlated with known aberrant ocular motor VSS metrics (shortened latencies and higher number of inhibitory errors) in VSS patients. Lastly, nodal co-modularity, a binary measure of node pairs belonging to the same module, was studied. VSS patients had lower modularity, supramarginal centrality and LE dynamics of multiple (sub)cortical regions, centered around occipital and parietal lobules. In VSS patients, lateral occipital cortex LE dynamics correlated positively with shortened prosaccade latencies ($p = .041$, $r = .353$). In VSS patients, occipital, parietal, and motor nodes belonged more often to the same module and demonstrated lower nodal co-modularity with temporal and frontal regions. This study revealed reduced dynamic variation in modularity and local efficiency strength in the VSS brain, suggesting that brain network dynamics are less variable in terms of segregation and local clustering. Further investigation of these changes could inform our understanding of the pathogenesis of the disorder and potentially lead to treatment strategies.

KEYWORDS

7 T MRI, network topology, ocular motor behavior, resting-state functional MRI, ultra-high field MRI, visual snow, visual snow syndrome

1 | INTRODUCTION

Visual snow syndrome (VSS) is a neurological disorder that manifests in dynamic visual disturbances across the entire visual field. Its

Scott C. Kolbe and Joanne Fielding contributed equally to this study.

This is an open access article under the terms of the [Creative Commons Attribution-NonCommercial-NoDerivs](https://creativecommons.org/licenses/by-nc-nd/4.0/) License, which permits use and distribution in any medium, provided the original work is properly cited, the use is non-commercial and no modifications or adaptations are made.

© 2022 The Authors. *Human Brain Mapping* published by Wiley Periodicals LLC.

defining feature, visual snow, is described as small flickering dots that are constantly present whether the eyes are open or closed. Visual snow is often accompanied by other visual symptoms such as enhanced entoptic phenomena, palinopsia, photophobia, and nyctalopia (Schankin et al., 2014). Diagnostic criteria involve visual snow and at least two of these other visual symptoms. In addition to visual symptoms, patients also experience a range of nonvisual sensory symptoms such as tinnitus and migraine as well as high rates of depression and anxiety, poor sleep quality, fatigue, and dissociative symptoms such as depersonalization (Solly et al., 2021). Collectively, these symptoms can severely impact a patient's daily life (Bou Ghannam & Pelak, 2017; Traber et al., 2020). We have also demonstrated alterations to eye movements in those with VSS, such as shortened latencies toward visual stimuli (prosaccade latencies) and decreased ability to inhibit eye movements to nontarget stimuli (antisaccade errors) (Solly et al., 2020). At present, the underlying neural functional mechanisms governing the visual changes are unclear.

In VSS patients, widespread structural brain changes have been reported (Michels et al., 2021; Puledda, Bruchhage, et al., 2020; Schankin et al., 2020; Strik et al., 2022) with occipital gray matter regions most strongly affected, followed by temporal, parietal, and frontal areas (Strik et al., 2022). While widespread structural involvement might be expected to manifest in alterations in brain function, the neuroimaging literature supporting this is still limited. Reduced activation upon presentation of visual snow like stimuli and hypermetabolism in the lingual gyrus have been reported using task fMRI and [18F]-FDG PET, respectively (Puledda, Ffytche, et al., 2020). At rest, disrupted connectivity has been found within multiple brain networks including visual, salience, and attention networks, although the direction of effect has been inconsistent, including both increased and decreased connectivity (Aldusary et al., 2020; Puledda et al., 2021). Instead of investigating individual regions and the connectivity between separated brain regions in isolation, we propose a more holistic view, studying the entire brain as a network. Simple inferences from highly complex systems can be derived using a network approach. Understanding how brain regions work together (network topology) may lead to greater insights into the pathophysiology of VSS. This has not been investigated previously. Specifically, we aimed to study two fundamental aspects of a network: network integration and network segregation. Network segregation was studied by evaluating modularity, recognizing that the brain naturally divides into communities that are strongly connected among themselves but sparsely connected with others, and local efficiency (i.e., the degree to which neighbor regions cluster together). Markers of network integration included eigenvector centrality (measure of a region's importance within a network) and global efficiency (connectedness of regions with other regions).

Alterations to brain network topology dynamics were characterized in VSS patients using high-resolution (7 T) functional MRI. Notably, dynamic connectivity is becoming an increasingly popular method for identifying differences in network switching in healthy and pathological brains. Instead of investigating connectivity and network topology over the entire scan duration and calculating an average, investigating dynamics characterizes fluctuation of a metric over time.

Given the wide variety of changes in brain microstructure (Strik et al., 2022), functional connectivity (Puledda et al., 2021) as well as range of symptoms (Solly et al., 2021) in VSS, we hypothesized that VSS patients would exhibit disrupted network topology dynamics at both a global and local level that would be related to ocular motor processing changes previously revealed in these individuals (Solly et al., 2020).

2 | METHODS

2.1 | Participants

Study approval was granted by Monash University Human Research Ethics Committee, and all participants gave voluntary, written informed consent prior to participation.

Sixty healthy controls (35 [58%] females; age = 32.0 ± 9.2 years) and 40 patients with VSS (21 [53%] females; age = 33.2 ± 10.1 years; 22 with migraines) were recruited using various forms of advertising (word-of-mouth, online, television, and radio). All patients met diagnostic criteria for VSS according to the International Classification of Headache Disorders (3rd edition; Table 1). Similar numbers of patients with ($n = 22$; 14 females; age = 34.7 ± 10.5 years) and without a history of migraine ($n = 17$; 7 females; age = 31.6 ± 9.7 years, 15 with visual aura) were included. To further ensure behavioral and MRI assessments were not affected by a migraine or migraine aura symptoms, participants were excluded where they experienced a migraine 3 days prior, during or up to 3 days after assessment. Additional exclusion criteria were a history or presence of a neurological disorder other than VSS or confounding psychiatric or ophthalmological conditions (assessed using a full ophthalmic examination; color vision, visual acuity, retinal structure, and retinal function).

As to medical history and medication use, patients were asked whether they had ever been diagnosed with a psychiatric and neurological conditions and whether they were currently using any medication. Out of 40, 25 patients reported comorbidities, either recently

TABLE 1 International Classification of Headache Disorders–3 criteria for a diagnosis of visual snow

- | |
|---|
| A. Dynamic, continuous, tiny dots across the entire visual field, persisting for >3 months |
| B. Additional visual symptoms of at least two of the following four types: <ol style="list-style-type: none"> 1. Palinopsia 2. Enhanced entoptic phenomena 3. Photophobia 4. Impaired night vision (nyctalopia) |
| C. Symptoms are not consistent with typical migraine visual aura |
| D. Symptoms are not better accounted for by another disorder |

Note: Diagnostic criteria involved visual snow >3 months, at least two other visual symptoms (palinopsia, enhanced entoptic phenomena, photophobia, nyctalopia), and symptoms not consistent with typical migraine visual aura or better accounted for by another disease.

diagnosed or no longer meeting diagnostic criteria. Comorbidities included mostly depression (12/40) and anxiety (16/40). However, attention deficit hyperactivity disorder (4/40), obsessive compulsive disorder (2/40), complex posttraumatic stress disorder (1/40), borderline personality disorder (1/40), vestibular condition (unspecified) (1/40), and dyslexia (1/40) were also self-reported. The vast majority did not report taking any medication. Only one VSS patient reported taking preventative migraine medication and five were taking anxiety/depression medication (5/19). Seven participants (out of 40) reported illicit drug use in the past, of which five did not report illicit drug use within 12 months prior to VSS onset, one after VSS onset, and one reported lifelong VSS. None of the participants reported illicit drug use within a week before testing.

2.2 | Ocular motor measures of visual processing

Visual processing was examined using two ocular motor tasks: prosaccade (PS) and antisaccade (AS) task. These tasks required the generation of a saccade toward a suddenly appearing stimulus (PS) or to its mirror opposite location (AS), the latter being more cognitively challenging. Previously, we revealed an ocular motor profile in VSS patients consistent with an alteration to the processing of visual stimuli (Solly et al., 2020). Specifically, VSS patients generated a speeded response to a suddenly appearing visual stimulus (PS, $p = .029$) and poorly suppressed a response to a suddenly appearing nontarget visual stimulus (AS, $p < .001$). A more detailed description of the tasks and findings can be found in the study by Solly et al. (2020)

2.3 | Imaging acquisition

Brain imaging was performed using a whole-body Siemens MAGNETOM 7 T MRI system (Siemens Healthcare, Erlangen, Germany) with a combined single-channel transmit and 32-channel receive head coil (Nova Medical, Wilmington, MA, USA). High temporal and spatial resolution resting-state fMRI (visual fixation on cross) were acquired in an axial plane using a multiband multislice gradient echo, echo planar sequence (Moeller et al., 2010) with the following parameters: repetition time (TR) = 800 ms, echo time (TE) = 22.2 ms, flip angle (FA) = 45 degrees, 84 slices, multiband factor = 6, acceleration factor (AF) = 2, phase encoding direction (PE) = anterior-to-posterior (AP), voxel size = 1.6 mm isotropic, image matrix = 130 × 130.

High-resolution anatomical images were acquired using a three-dimensional T₁-weighted sequence (MP2RAGE: TR = 5000 ms, TE = 3.06 ms, inversion time = 700/2700 ms, FA = 4°/5°, 224 slices, AF = 4, PE = AP, voxel size = 0.75 mm isotropic, image matrix = 330 × 330, imaging plane = sagittal).

2.4 | Functional resting-state MRI preprocessing

Resting-state fMRI data were preprocessed using MELODIC using standard settings (part of FSL5, FMRIB 2012, Oxford, UK; [\[fsl.fmrrib.ox.ac.uk/fsl/\]\(https://fsl.fmrrib.ox.ac.uk/fsl/\)\) and involved head motion correction \(MCFLIRT\), brain extraction \(BET\), spatial smoothing with a 3.2 mm \(double the voxel size\) full width at half-maximum Gaussian kernel and temporal filtering including a high-pass filter with a 100 s cut-off \(equivalent to 0.01 Hz\). In addition to temporal filtering, voxel signal time courses were corrected for mean white matter and cerebrospinal fluid time course using linear regression to account for global signal variations during scanning sessions. To further minimize motion effects on the fMRI, signal additional motion correction steps were performed using FIX \(part of FSL5, FMRIB 2012, Oxford, UK, <https://fsl.fmrrib.ox.ac.uk/fsl/>\). FIX was trained using the independent component analysis \(ICA\) data sets ran by MELODIC in subset of subjects. For those subjects the components were manually classified into “good” and “bad.” Subsequently, the new trained-weights files were used to classify components in the remaining subjects' datasets and to refine the data.](https://fsl.fmr</p></div><div data-bbox=)

2.5 | Regions of interest and network computation

Regions of interest (ROI) were chosen based on a recent publication showing widespread (sub)cortical structural changes (Strik et al., 2022). To keep analyses consistent and explorative, similar ROIs were used. Cortical (68) and subcortical (14) ROIs were segmented using each individual uniform denoised MP2RAGE image and FreeSurfer (v.6.0-patch; <https://surfer.nmr.mgh.harvard.edu/>, Figure 1). Segmentations were visually checked and manually edited if needed. Regions were warped to fMRI subject space using transformation matrices calculated using bbgregister (FreeSurfer, v.6.0-patch) and FLIRT (part of FSL6, fsl.fmrrib.ox.ac.uk). Connectivity and network analyses performed using customized MATLAB R2022a (Mathworks, Natick, MA, USA) scripts. Preprocessed RS fMRI signals were extracted from FreeSurfer parcellated cortex and subcortical gray matter. Connectivity between each ROI pair was computed as a pairwise correlation coefficient, resulting in an 82 by 82 matrix (Figure 1).

Network metrics were calculated using the Brain Connectivity Toolbox (<https://sites.google.com/site/bctnet/>). Network integration was studied using global efficiency and eigenvector centrality and network segregation was investigated using modularity and local efficiency. Global efficiency was calculated using the inverse of the average shortest pathlength, that is, number of steps required to connect ROIs. Network modularity (Q) was assessed using the Newman's algorithm, which calculates the optimal number of modules by repeatedly subdividing the network until connectivity within and between modules is similar to a randomly reconnected network. When a split results in a negative or zero contribution to Q the maximum Q is reached and the entire network has been decomposed into indivisible modules (Newman, 2006). Local network metrics computed included the local efficiency, related to the degree to which ROIs cluster together, and eigenvector centrality, a measure of importance within a network.

To assess the dynamics of these network metrics, correlations and network metric computation was performed in sliding windows of 20 timepoints (16 s) and a shift length of 5 timepoints (4 s) across the

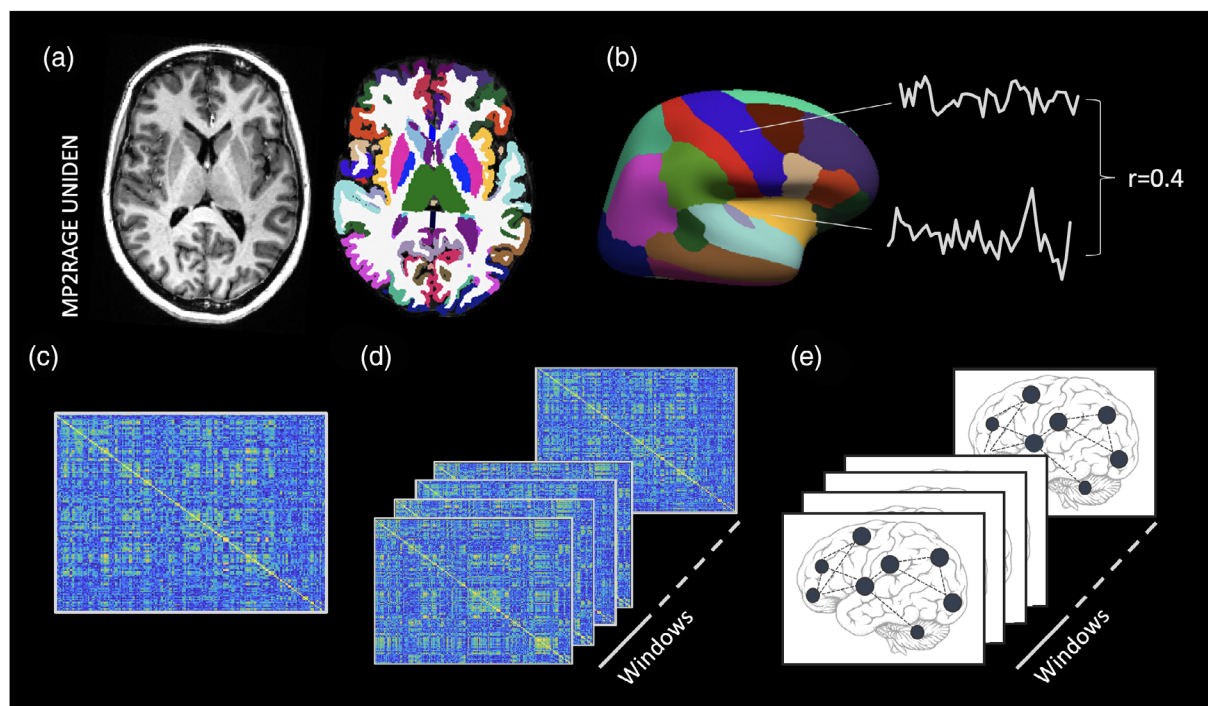


FIGURE 1 Overview network analyses pipeline. (a) High-resolution structural images were used for cortical and subcortical segmentation analyses using FreeSurfer. (b) Preprocessed fMRI signals were extracted from regions of interest and connectivity between node pairs was calculated using correlation coefficients, (c) resulting in a connectivity matrix. (d) A dynamic approach was used, and correlations were performed in sliding windows of 16 s (20 volumes) across the acquisition (shift length of 5 volumes), resulting in 76 windows. (e) Network metrics were calculated for each window and dynamics defined as the coefficient of variation over time.

acquisition ($82 \times 82 \times 76$). Dynamics was defined as the coefficient of variation over time for each network metric, that is, the standard deviation over time divided by the mean over time.

To further investigate modularity in the brain, we explored whether modules were more rigid or flexible in their composition in VSS patients. To do this, we calculated a novel metric, nodal co-modularity. For each node pair, the nodal co-modularity was calculated, which is binary and equal to one when two nodes belong to the same module and zero when two nodes belong to different modules. The nodal co-modularities were averaged across subjects in healthy controls and patients.

2.6 | Statistical analyses

All statistical analyses were performed using MATLAB Statistic Toolbox (R2022a, MathWorks, MA, USA) using a critical p value threshold of .05 (Benjamini & Hochberg, 1995). Demographic variables were compared between groups using independent samples t -tests, or Mann-Whitney U-tests for non-normally distributed data and Chi-square test for nominal variables. Dynamic modularity, global efficiency, local efficiency, and eigenvector centrality were compared between VSS patients and controls using independent sample t -tests. Significant MRI measures were correlated with behavioral variables PS latency and AS errors and included age as covariate using Pearson

correlations for normally distributed data and Spearman for non-normally distributed data. To study the potential influence of comorbid migraine, significant network metrics were compared between patients with and without migraine using independent sample t -tests. Nodal co-modularity was visually compared between groups.

3 | RESULTS

3.1 | Demographic and clinical characteristics

Demographic and clinical characteristics are shown in Table 2. No differences were found between controls and VSS patients on any demographic variable. The demographics and clinical characteristics did not differ between VSS patients with and without migraines and were therefore combined to one group.

3.2 | Network metrics dynamics

On a global level, VSS patients demonstrated reduced dynamic variation in modularity strength over time. On a local level, reduced left supramarginal centrality dynamics was observed, as well as reduced local efficiency dynamics of multiple (sub)cortical regions, centered around the occipital, temporal, and parietal lobules (Figure 2). Regions

TABLE 2 Demographic and visual snow symptoms

Controls	Controls	VSS		VSS without migraine	VSS with migraine	
Demographics			<i>p</i> value			<i>p</i> value
Participants, <i>n</i>	60	40		17	22	
Age, years	32.24 (8.89)	33.18 (10.08)	.877	31.55 (9.69)	34.69 (10.54)	.322
Sex, female/male	35/25	21/19	.681	7/10	14/8	.206
Visual snow symptoms						
Disease duration, years		20.10 (12.65)		18.59 (12.25)	20.96 (13.33)	.504
Lifelong VSS / sudden onset		15/21		6/9	9/12	
Age of onset if not lifelong, years		23.24 (10.12)		23.11 (10.81)	23.33 (10.07)	.831
Visual symptoms ^a (out of 8)		5.33 (1–8)		5.13 (1–8)	5.48 (3–8)	.858
After images, y/n		7/29		11/4	18/3	
Trailing moving objects, y/n		14/22		11/4	11/10	
Nyctalopia, y/n		13/23		11/4	12/9	
Photophobia, y/n		19/17		6/9	11/10	
Floaters, y/n		4/32		13/2	19/2	
Blue field EP, y/n		10/26		9/6	17/4	
Self-lightning, y/n		20/16		7/8	9/12	
Halos, y/n		9/27		9/6	18/3	
Sensory symptoms ^a (out of 4)		1.36 (0–4)		1.53 (0–3)	1.24 (0–4)	.343
Tinnitus, y/n		13/23		9/6	14/7	
Paraesthesia, y/n		21/15		8/7	7/14	
Tremors, y/n		29/7		4/11	3/18	
Dizziness, y/n		32/4		2/13	2/19	
Family history VS, y/n		1/35		0/15	1/20	
Family history migraine, y/n		20/16		5/10	15/6	
Migraine with visual aura, y/n		15/6			15/6	

Note: Values are means and standard deviations unless indicated otherwise.

Abbreviations: n, no; VSS, visual snow syndrome; y, yes.

^aSelf-rating scores are mean and range.

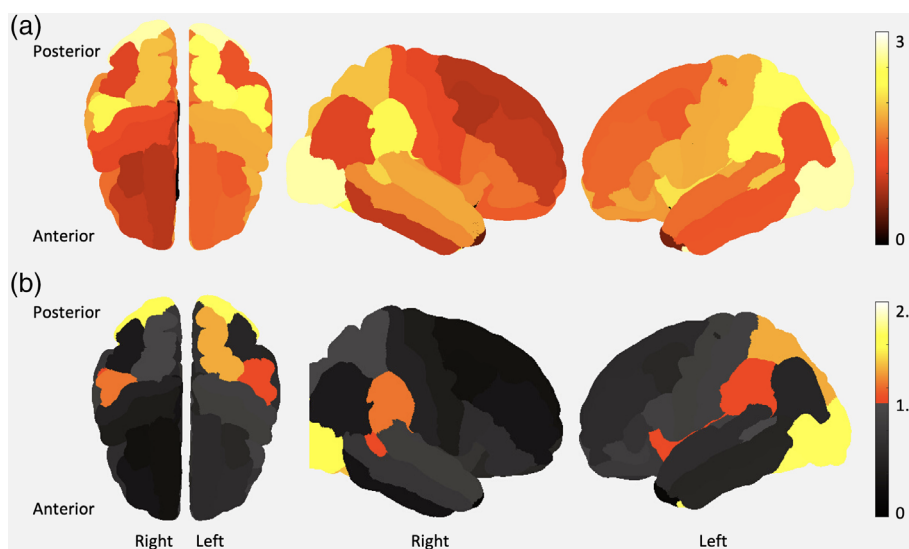


FIGURE 2 Reduced network dynamics in VSS patients. Resting-state network dynamics was significantly reduced in VSS patients. (a) Cortical regions are colored with the effect size. (b) Areas of significant differences are colored with p values ($-\log_{10}$). Significant differences were observed in occipital, parietal, temporal regions, with primary visual processing areas showing the strongest effect.

with reduced local efficiency dynamics included right and left fusiform, lateral occipital cortex, parahippocampal cortex, supramarginal gyrus, right banks of the superior temporal sulcus and pallidum, left

insula, superior parietal cortex, cerebellar cortex and putamen (Figure 2). These network metrics did not significantly differ between VSS patients with and without migraines.

3.3 | Correlation with visual processing

In VSS patients, lower local efficiency dynamics of the left lateral occipital cortex correlated with shorter prosaccade latencies ($p = .041, r = .353$).

3.4 | Nodal co-modularity

In VSS patients, occipital, parietal, and primary somatosensory and motor nodes belonged more often to the same module and demonstrated lower nodal co-modularity with temporal and frontal regions (Figure 3).

4 | DISCUSSION

This study investigated functional brain network abnormalities in people with VSS, revealing reduced network dynamics at a global and local level. VSS patients demonstrated reduced variation in modularity, eigenvector centrality, and local efficiency strength, suggesting disturbed processes of integration and segregation. Abnormal dynamic local efficiency was observed in parietal cortices, temporal cortices, cerebellum as well as the deep gray matter regions, with the strongest impact in the occipital cortex. Of these network changes, the lateral occipital cortex efficiency dynamics was related to ocular motor responses previously shown to dissociate VSS patients from neurologically healthy individuals (shortened prosaccade latencies).

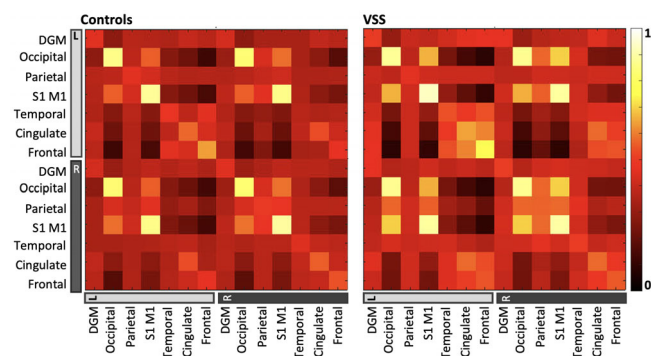


FIGURE 3 Conodal modularity. Conodal modularity matrices for controls (left) and VSS patients (right). The color of each node pair indicates the proportion of subjects where node pairs were members of the same module. The most noticeable difference between groups is for nodal co-modularity in occipital, parietal and primary motor areas. Nodal co-modularity is highest in these regions, suggesting that these nodes belong more often to the same module in VSS patients. However, the opposite was seen between nodes in these networks and frontal and cingulate areas, suggesting these node pairs belong less often to the same module. DGM, deep gray matter; S1, primary somatosensory cortex; M1, primary motor cortex

4.1 | Disrupted network dynamics

The brain is a complex system that is highly connected. To simplify this complexity, the brain can be viewed as a network. Network science has been increasingly applied over the last years and revealed meaningful information about the effects of pathology on the organization of complex networks in the brain and the dynamic nature and adaptivity of these systems. In this study, we identified functional network disturbances in VSS patients. Specifically, in VSS patients, measures of network integration (eigenvector centrality) and network segregation (local efficiency and modularity) were both affected, indicating less flexibility in basal and essential aspects of a network. The VSS literature on brain connectivity and networks is still limited. A recent VSS study investigated static (over entire scan) network connectivity disruptions and reported higher and lower connectivity within several networks including visual, default mode, salience and attention networks at rest, as well as during visual snow like stimulation task, suggesting widespread disrupted connectivity (Puledda et al., 2021). However, it remains unclear what the impact of this hyper- and hypo connectivity is on VSS symptomatology, overall brain network topology and the stability of a network (the temporal fluctuations within the scan). In regard to network stability, dynamics have recently been used and validated in various neurological diseases such as multiple sclerosis (Eijlers et al., 2019; Fuchs et al., 2022) and migraine (Tu et al., 2019) with differences in how networks switch in pathological brains evident relative to healthy brains. In particular, in multiple sclerosis, lower and greater network dynamics have been concurrently observed and found to be related to clinical disability (Eijlers et al., 2019; Fuchs et al., 2022), leading to the suggestion that networks are inflexible and or unstable. In both situations, a network seems to be unable to perform as needed. A recent study in migraine (Tu et al., 2019), a common comorbidity of VSS, focused on the thalamocortical dynamics of five different brain states and reported altered global and local efficiency dynamics in a specific state. In this study, we observed a trend toward lower global efficiency dynamics and reduced local efficiency dynamics in multiple regions in VSS patients. To study the effects of migraine, we compared network metrics between VSS patients with and without migraine and observed no differences, suggesting that the functional dynamic alterations found were VSS specific.

4.2 | The role of the occipital cortices and visual processing

VSS patients demonstrated altered network dynamics at a global and local level with reduced local efficiency dynamics centered around temporal, parietal, and occipital areas. Reduced variability of local efficiency was the strongest in visual areas and related to aberrant visual processing in VSS patients, suggesting a specific role of the visual processing regions in VSS. The involvement of visual areas has been demonstrated in several previous reports (Chen et al., 2011;

Michels et al., 2021; Puledda et al., 2021; Puledda, Bruchhage, et al., 2020; Schankin et al., 2020). In addition, we recently reported widespread microstructural gray matter changes in VSS, with the occipital cortices affected most profoundly (Strik et al., 2022). While the anatomical effects were robust and widespread, functionally differences seem to be more subtle but centered again around the occipital cortices and related to visual processing. Specifically, shorter prosaccade latencies (Solly et al., 2020) correlated with lower local efficiency dynamics of the lateral occipital cortex, a visual processing area involved in object recognition and visual-spatial processing. Although the underlying mechanisms of VSS remain unclear, cortical hyperexcitability of visual processing areas is a common theory (Bou Ghannam & Pelak, 2017; McKendrick et al., 2017) and appears consistent with our findings. As reported previously, VSS patients demonstrate a speeded prosaccade response in reaction to a suddenly appearing visual stimuli (Solly et al., 2020). Hyperexcitability could lead to abnormal network dynamics of the lateral occipital cortex, which may lead to accelerated initial processing of a visual stimulus.

In addition, disturbed visual attention processes could also account for the findings, with network inflexibility leading to inappropriate attention and/or feedback loops, resulting in speeded visual processing and commensurate responses. This attention hypothesis is supported by previous research demonstrating functional activation changes within the anterior insula in response to a VS-like task, hypothesized to be due to disturbances within the salience network, a network involved in attention to visual stimuli (Puledda, Ffytche, et al., 2020). A more recent study reported connectivity disruption within the salience and attention networks when processing external stimulus (Puledda et al., 2021). In this study, we observed reduced modularity dynamics, that is, less fluctuation in modularity strength over time. This suggests less switching in the division of modules. We also visually explored whether modules were more rigid in their composition by calculating how often nodes belonged to the same module. We observed lower nodal co-modularity between occipital, parietal, and sensorimotor nodes and frontal and cingulate regions. Together, these results suggest visual processing areas and more fundamental processes such as attention are disrupted and potentially disjointed in VSS, which might explain their shorter prosaccade latencies results (Solly et al., 2020). Shorter prosaccade latencies indicates that the initial processing of a visual stimuli might be accelerated due to enhanced attentional capture. Potentially the thalamus, an important relay center in the brain, may play an essential role as suggested by previous research (Lauschke et al., 2016; Tu et al., 2019; Vanneste et al., 2018). The thalamus is widely connected to cortical areas and disruption to thalamocortical loops may influence the speed at which a visual image is processed and responded to. In this study, no network disturbances were found for the thalamus specifically; however, a more focused study investigating both the structural and functional network connectivity of the thalamus might lead to more insights of the neuronal mechanisms underlying VSS.

4.3 | Limitations and future directions

There are several limitations, challenges and future directions that need to be considered. While the sample size is moderately large, future studies including more patients may provide the opportunity to assess distinct groups and provide more generalizable results. Subdividing patients into lifelong and a sudden onset of VSS and or a longitudinal design may provide insight into the cause and or potential progression of VSS. Specific network patterns may be evident and important predictors of conversion to and progression of VSS. While many different network measures can be calculated, we chose to investigate four different metrics to assess network integration and segregation. Besides global and local efficiency, a measure of information propagation, we chose to explore modularity and centrality, metrics indicating “importance” of regions. Other metrics and or a static approach could provide additional insight into the pathological mechanisms of VSS, what might be explored in future studies. In addition, instead of studying the brain at rest, functional changes might be more prominent during a visual task. Research is still limited, and areas found to be involved are relatively small (Puledda et al., 2021; Puledda, Ffytche, et al., 2020). Investigating ocular motor performance while acquiring functional brain activity may provide more direct and accurate measures of visual processing and lead to the provision of greater insights into the functional mechanisms underlying VSS. Similarly, while no structural hemispheric dominance was observed in a recent paper (Strik et al., 2022), some functional changes were observed in either hemisphere (Strik et al., 2022). The relation between structural and functional network connectivity and topology might provide more insight.

5 | CONCLUSION

This study revealed alterations to brain network topology dynamics in VSS patients at a global and local level, centered around occipital cortices, related to ocular motor processing changes. Reduced variation in modularity and local efficiency strength over time, suggest that brain networks are less variable in terms of segregation and local clustering in VSS. Further investigation of these functional changes could provide additional information to the underlying mechanisms of the disorder and potentially lead to treatment strategies.

ACKNOWLEDGMENTS

The authors acknowledge the facilities, scientific and technical assistance from the National Imaging Facility, a National Collaborative Research Infrastructure Strategy capability, at the Melbourne Brain Centre Imaging Unit, The University of Melbourne. This work was supported by a research collaboration agreement with Siemens Healthineers. The authors would like to thank Professor Carsten Murawski and Mr Juan Pablo Franco from the Brain, Mind and Markets Laboratory at the University of Melbourne for contributing healthy control data for this study. This work was supported by the MASSIVE HPC facility (www.massive.org.au).

CONFLICT OF INTEREST

The authors report no competing interests.

DATA AVAILABILITY STATEMENT

Data reported in this manuscript can be made available by the corresponding author on reasonable request.

ORCID

Myrte Strik  <https://orcid.org/0000-0001-8995-9899>

Emma J. Solly  <https://orcid.org/0000-0002-5241-6572>

Rebecca Glarin  <https://orcid.org/0000-0003-0343-8537>

Owen B. White  <https://orcid.org/0000-0002-2836-7344>

Scott C. Kolbe  <https://orcid.org/0000-0003-4685-1380>

Joanne Fielding  <https://orcid.org/0000-0002-1131-0587>

REFERENCES

- Aldusary, N., Traber, G. L., Freund, P., Fierz, F. C., Weber, K. P., Baeshen, A., Alghamdi, J., Saliju, B., Pazahr, S., Mazloum, R., Alshehri, F., Landau, K., Kollias, S., Piccirelli, M., & Michels, L. (2020). Abnormal connectivity and brain structure in patients with visual snow. *Frontiers in Human Neuroscience*, 14, 476. <https://doi.org/10.3389/FNHUM.2020.582031/XML/NLM>
- Benjamini, Y., & Hochberg, Y. (1995). Controlling the false discovery rate: A practical and powerful approach to multiple testing. *Journal of the Royal Statistical Society: Series B (Methodological)*, 57(1), 289–300. <https://doi.org/10.1111/j.2517-6161.1995.tb02031.x>
- Bou Ghannam, A., & Pelak, V. S. (2017). Visual snow: A potential cortical hyperexcitability syndrome. *Current Treatment Options in Neurology*, 19(3), 9. <https://doi.org/10.1007/s11940-017-0448-3>
- Chen, W. T., Lin, Y. Y., Fuh, J. L., Hämäläinen, M. S., Ko, Y. C., & Wang, S. J. (2011). Sustained visual cortex hyperexcitability in migraine with persistent visual aura. *Brain*, 134(8), 2387–2395. <https://doi.org/10.1093/brain/awr157>
- Eijlers, A. J. C., Wink, A. M., Meijer, K. A., Douw, L., Geurts, J. J. G., & Schoonheim, M. M. (2019). Reduced network dynamics on functional MRI signals cognitive impairment in multiple sclerosis. *Radiology*, 292(2), 449–457. <https://doi.org/10.1148/radiol.2019182623>
- Fuchs, T. A., Schoonheim, M. M., Broeders, T. A. A., Hulst, H. E., Weinstock-Guttman, B., Jakimovski, D., Silver, J., Zivadinov, R., Geurts, J. J. G., Dwyer, M. G., & Benedict, R. H. B. (2022). Functional network dynamics and decreased conscientiousness in multiple sclerosis. *Journal of Neurology*, 269(5), 2696–2706. <https://doi.org/10.1007/S00415-021-10860-8/FIGURES/3>
- Lauschke, J. L., Plant, G. T., & Fraser, C. L. (2016). Visual snow: A thalamocortical dysrhythmia of the visual pathway? *Journal of Clinical Neuroscience*, 28, 123–127. <https://doi.org/10.1016/j.jocn.2015.12.001>
- McKendrick, A. M., Chan, Y. M., Tien, M., Millist, L., Clough, M., Mack, H., Fielding, J., & White, O. B. (2017). Behavioral measures of cortical hyperexcitability assessed in people who experience visual snow. *Neurology*, 88(13), 1243–1249. <https://doi.org/10.1212/WNL.0000000000003784>
- Michels, L., Stämpfli, P., Aldusary, N., Piccirelli, M., Freund, P., Weber, K. P., Fierz, F. C., Kollias, S., & Traber, G. (2021). Widespread white matter alterations in patients with visual snow syndrome. *Frontiers in Neurology*, 12, 41–49. <https://doi.org/10.3389/fneur.2021.723805>
- Moeller, S., Yacoub, E., Olman, C. A., Auerbach, E., Strupp, J., Harel, N., & Ugurbil, K. (2010). Multiband multislice GE-EPI at 7 tesla, with 16-fold acceleration using partial parallel imaging with application to high spatial and temporal whole-brain fMRI. *Magnetic Resonance in Medicine*, 63(5), 1144–1153. <https://doi.org/10.1002/mrm.22361>
- Newman, M. E. J. (2006). Modularity and community structure in networks. *Proceedings of the National Academy of Sciences*, 103(23), 8577–8582. <https://doi.org/10.1073/pnas.0601602103>
- Puledda, F., Bruchhage, M., O'Daly, O., Ffytche, D., Williams, S. C. R., & Goadsby, P. J. (2020). Occipital cortex and cerebellum gray matter changes in visual snow syndrome. *Neurology*, 95(13), e1792–e1799. <https://doi.org/10.1212/WNL.0000000000010530>
- Puledda, F., Ffytche, D., Lythgoe, D. J., O'Daly, O., Schankin, C., Williams, S. C. R., & Goadsby, P. J. (2020). Insular and occipital changes in visual snow syndrome: A BOLD fMRI and MRS study. *Annals of Clinical Translational Neurology*, 7(3), 296–306. <https://doi.org/10.1002/acn3.50986>
- Puledda, F., O'Daly, O., Schankin, C., Ffytche, D., Williams, S. C. R., & Goadsby, P. J. (2021). Disrupted connectivity within visual, attentional and salience networks in the visual snow syndrome. *Human Brain Mapping*, 42(7), 2032–2044. <https://doi.org/10.1002/hbm.25343>
- Schankin, C. J., Maniyar, F. H., Chou, D. E., Eller, M., Sprenger, T., & Goadsby, P. J. (2020). Structural and functional footprint of visual snow syndrome. *Brain*, 143(3), 1106–1113. <https://doi.org/10.1093/brain/awaa053>
- Schankin, C. J., Maniyar, F. H., Digre, K. B., & Goadsby, P. J. (2014). “Visual snow” - A disorder distinct from persistent migraine aura. *Brain*, 137(5), 1419–1428. <https://doi.org/10.1093/brain/awu050>
- Solly, E. J., Clough, M., Foletta, P., White, O. B., & Fielding, J. (2021). The psychiatric symptomatology of visual snow syndrome. *Frontiers in Neurology*, 12, 1–10. <https://doi.org/10.3389/fneur.2021.703006>
- Solly, E. J., Clough, M., McKendrick, A. M., Foletta, P., White, O. B., & Fielding, J. (2020). Ocular motor measures of visual processing changes in visual snow syndrome. *Neurology*, 95(13), e1784–e1791. <https://doi.org/10.1212/WNL.0000000000010372>
- Strik, M., Clough, M., Solly, E. J., Glarin, R., White, O. B., Kolbe, S. C., & Fielding, J. (2022). Microstructure in patients with visual snow syndrome: An ultra-high field morphological and quantitative MRI study. *Brain Communications*, 4(4), 1–9. <https://doi.org/10.1093/BRAINCOMMS/FCAC164>
- Traber, G. L., Piccirelli, M., & Michels, L. (2020). Visual snow syndrome: A review on diagnosis, pathophysiology, and treatment. *Current Opinion in Neurology*, 33(1), 74–78. <https://doi.org/10.1097/WCO.0000000000000768>
- Tu, Y., Fu, Z., Zeng, F., Maleki, N., Lan, L., Li, Z., Park, J., Wilson, G., Gao, Y., Liu, M., Calhoun, V., Liang, F., & Kong, J. (2019). Abnormal thalamocortical network dynamics in migraine. *Neurology*, 92(23), E2706–E2716. <https://doi.org/10.1212/WNL.0000000000007607>
- Vanneste, S., Song, J. J., & de Ridder, D. (2018). Thalamocortical dysrhythmia detected by machine learning. *Nature Communications*, 9(1), 1–13. <https://doi.org/10.1038/s41467-018-02820-0>

How to cite this article: Strik, M., Clough, M., Solly, E. J., Glarin, R., White, O. B., Kolbe, S. C., & Fielding, J. (2023). Brain network dynamics in people with visual snow syndrome. *Human Brain Mapping*, 44(5), 1868–1875. <https://doi.org/10.1002/hbm.26176>